Power-on Channel Wing Aerodynamics

EDWARD F. BLICK* AND VINCENT HOMER†
University of Oklahoma, Norman, Okla.

A theory is developed for lift developed by semicircular channel wings with a pusher propeller at the trailing edge. The theory assumes that the lift on the inside (or top) of a channel airfoil can be determined by using standard airfoil pressure coefficient data but with an effective freestream velocity and an effective freestream static pressure equal to those values just in front of the propeller plane. The lift on the outside (or bottom) of a channel airfoil is assumed to be the same as that calculated by present-day standard methods. Good correlation was found between the theory and wind-tunnel and flight-test data. Both the theory and test data indicate extremely large values of lift coefficient can be obtained with channel wings.

Nomenclature

A = area of propeller disk
A_e = streamtube area of infinity
c = wing chord length
C_l = lift coefficient/unit span
C_{li} = ideal lift coefficient/unit span
C_L = power-on lift coefficient, $L/q_\infty S$
$C_L{}^*$ = unpowered lift coefficient, $L/q_\infty S$
C_T = thrust coefficient, $T/q_\infty A$
L = lift
$\dot{m}$ = mass flow rate
n = number of engines
P = power
p = pressure
T = thrust/engine
T_c = thrust coefficient, $nT/q_\infty S$
q = dynamic pressure, $\frac{1}{2}\rho V^2$
R = channel radius
S = total horizontal projected wing area
S_c = horizontal projected channel wing area, $2Rc$
V = velocity
x = distance from leading edge along chord line
α = angle of attack
$\bar{\alpha}$ = average sectional angle of attack in the channel
$= \cos^{-1}\int_0^{\pi/2} \cos\alpha \cos\varphi \, d\varphi = \cos^{-1}[\alpha \cot\alpha]_{\varphi=0}$
ϵ = downwash angle
η = fraction of lift generated by lower surface
ρ = air density
φ = angle [see Fig. (3)]

Subscripts

c = channel
d = propeller disk
e = streamtube at downstream infinity
∞ = freestream
U = upper airfoil surface
L = lower airfoil surface
$w\text{-}c$ = wing − channel

Introduction

ALTHOUGH several full-scale channel wing aircraft have flown and demonstrated STOL capabilities since 1943, there has been a dearth of theoretical and experimental research applied toward this concept. Without doubt, this lack of satisfactory theory and design formulas for predicting lift on channel wings seriously impeded the development of channel wing aircraft. The major portion of this study is directed toward the development of a theory of power-on channel wing lift and correlation of the theory with experimental wind-tunnel and flight-test data.

Received May 18, 1970; revision received August 28, 1970.

* Professor, Department of Aerospace and Mechanical Engineering. Member AIAA.
† Senior, School of Aerospace and Mechanical Engineering. Student Member AIAA.

Static Channel Wing Lift

Consider the semicircular wing with propeller at the trailing edge plane (Fig. 1). Assume the forward speed of the channel wing is zero and assume a pusher propeller is inducing a flow through the channel. Assume that the capture area of the induced flow at infinity is A_e and assume that this flow is deflected uniformly by an angle ϵ at infinity downstream. The mass flow rate is

$$\dot{m} = \rho A_e V_e \tag{1}$$

By application of the momentum theorem, the lift is

$$L = \dot{m} V_e \sin\epsilon \tag{2}$$

The minimum possible power to produce this lift is obtained by equating the power to the kinetic energy of the induced flow,

$$P = \tfrac{1}{2}\dot{m} V_e{}^2 \tag{3}$$

Assuming lift equal weight ($L = W$), Eqs. (1–3) can be combined to obtain an equation for the power loading or ideal lift efficiency of a channel wing

$$W/P = 2(\rho)^{1/2} \sin^{3/2}\epsilon/(W/A_e) = 2\sin\epsilon/V_e \tag{4}$$

For the special case of the downwash angle ϵ equal to 90°, Eq. (4) reduces to the equation for the ideal hovering efficiency of a lifting rotor. If one assumes that the jet contraction behind the propeller of the channel wing behaves in similar fashion as a free propeller, then the well known Froude relation shows that $A_e = A/2$, where A is the area of the propeller disk. Hence, Eq. (4) can be written as

$$W/P = (2\rho)^{1/2} \sin^{3/2}/(W/A)^{1/2} \tag{5}$$

Equation (5) is plotted in Fig. 2 for the limiting case of ϵ equal to 90°. This would represent the theoretical upper limit of lift efficiency for a channel wing as well as any lifting rotor system. The experimental data indicate that the channel wing is a surprisingly efficient lift generator. The largest channel wing lift efficiency measured, 13.7 lb/hp, is in the same range as those generated by helicopters. Even though the static lift efficiencies of the channel wings are large, problems associated with control would probably prove to be serious barriers to overcome in trying to develop VTOL channel wing aircraft. However the prospects of developing STOL aircraft using channel wings does look promising.

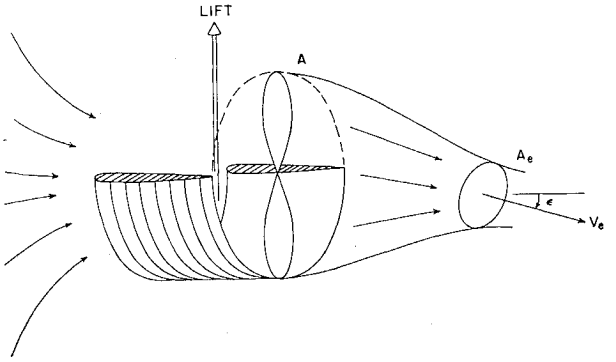

Fig. 1 Channel wing lift at zero forward speed.

Forward Flight Channel Wing Lift

The hypothesis is made that the first-order approximation to the flow through a semicircular channel wing with propeller (see Fig. 3) is similar to that of flow through an isolated propeller. The well known Froude relation shows that the slipstream velocity is twice the mean velocity through the propeller disk. In addition, the momentum theory can be used to show the relation between the velocity at the propeller disk and the freestream velocity,[8]

$$V_d/V_\infty = (q_d/q_\infty)^{1/2} = \tfrac{1}{2}[1 + (1 + C_T)^{1/2}] \quad (6)$$

Writing the Bernoulli equation for a streamline between upstream infinity and a point just in front of the propeller disk, one obtains,

$$p_\infty - p_d = \tfrac{1}{2}\rho V_\infty^2[(V_d/V_\infty)^2 - 1] = q_\infty[q_d/q_\infty - 1] \quad (7)$$

Writing the Bernoulli equation for a streamline between an arbitrary point on the upper (or inside) surface of the channel and a point just in front of the propeller disk (trailing edge), one obtains,

$$p - p_d = \tfrac{1}{2}\rho V_d^2[1 - (V/V_d)^2] \quad (8)$$

Or the pressure coefficient on the upper channel surface can be expressed for the power-on condition as

$$C_{pU} = (p - p_d)/\tfrac{1}{2}\rho V_d^2 \quad (9)$$

Since the pressure coefficient on an airfoil in a uniform flow is independent of freestream static pressure or freestream velocity then additionally one can write

$$C_{pU} = (p - p_\infty)/\tfrac{1}{2}\rho V_\infty^2 \quad (10)$$

Thus, it is hypothesized that the flow on the top side of the channel with pusher propeller is equivalent to that of an unpowered (no propeller) channel with a freestream velocity V_d and a freestream static pressure p_d.

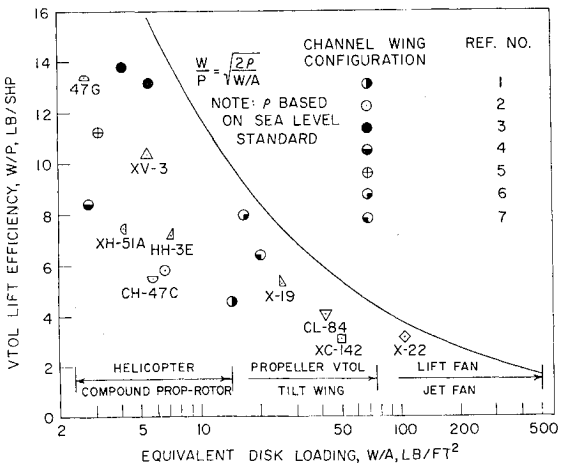

Fig. 2 Comparison of vertical lift efficiencies.

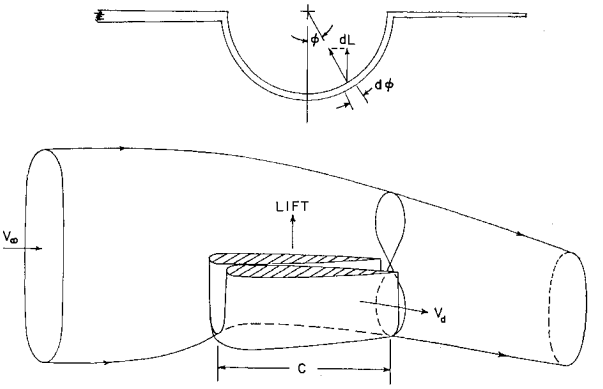

Fig. 3 Channel wing lift at forward speed V_∞.

For a slender airfoil section the lift on the channel can be expressed as

$$L_c = \int_{\pi/2}^{\pi/2} \cos\alpha \cos\varphi \int_0^c [-(p - p_\infty)_U + (p - p_\infty)_L](dx)R(d\varphi) \quad (11)$$

The local section angle of attack is given by $\alpha = \tan^{-1}(\cos\varphi \tan\alpha_{\varphi=0})$. With the help of Eqs. (9) and (10), Eq. (11) can be reduced to

$$L_c = (2Rc)\cos\bar{\alpha} \int_0^1 [-C_{pU}q_d + C_{pL}q_\infty + (p_\infty - p_d)]d(x/c) \quad (12)$$

Using Eq. (7), Eq. (12) can be expressed as

$$L_c = (1 - \eta)C_L^* q_d S_c + \eta C_L^* q_\infty S_c + (q_d - q_\infty)S_c \cos\bar{\alpha} \quad (13)$$

where

η = fraction of lift generated by lower surface of airfoil
$= \dfrac{\cos\bar{\alpha}}{C_L^*} \int_0^1 C_{pL} \dfrac{dx}{c}$

$1 - \eta$ = fraction of lift generated by upper surface of airfoil

C_L^* = power-off channel wing lift coefficient
$= \cos\bar{\alpha} \int_0^1 (-C_{pU} + C_{pL}) \dfrac{dx}{c}$

S_c = horizontal projected channel wing area
$= 2Rc$

Figure 4 illustrates the fraction of lift generated by the upper surface for several different airfoils (see Appendix for the derivation of η).

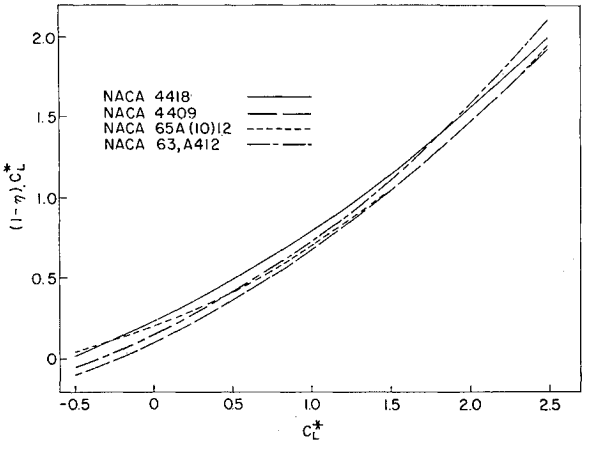

Fig. 4 Lift coefficient on upper surface of airfoils.

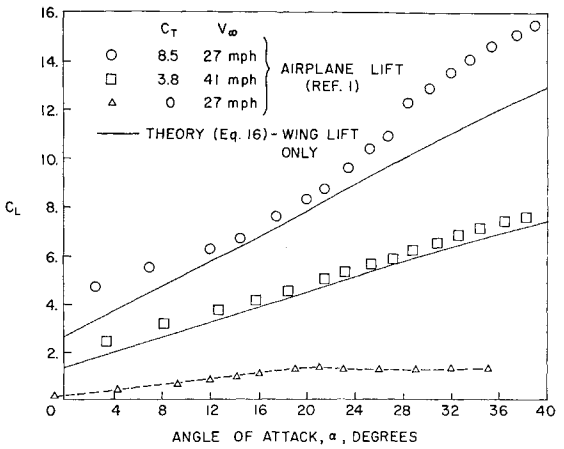

Fig. 5 Comparison between theory and full-scale wind-tunnel data.

If the wing is equipped with planar wings connected to the ends of the channel, then the lift on the nonchannel portion of the wing can be expressed as

$$L_{w-c} = (C_L^*)_{w-c} q_\infty (S - S_c) \tag{14}$$

Now by adding Eq. (14) and the lift component of the propeller thrust ($T \sin\alpha$) to Eq. (13) the total lift generated by the wing is

$$L = (1 - \eta) C_L^* q_d S_c + \eta C_L^* q_\infty S_c + (C_L^*)_{w-c} q_\infty (S - S_c) + (q_d - q_\infty) S_c \cos\bar{\alpha} + nT \sin\alpha \tag{15}$$

Basing the over-all power-on lift coefficient on the horizontal projected wing area S and the freestream dynamic pressure q_∞, Eq. (15) can be rearranged with the help of Eq. (6) to obtain,

$$C_L = C_L^*(S_c/S)[(1 - \eta)(\tfrac{1}{4})[1 + (1 + C_T)^{1/2}]^2 + \eta] + (C_L^*)_{w-c}(1 - S_c/S) + [\tfrac{1}{4}[1 + (1 + C_T)^{1/2}]^2 - 1](S_c/S) \cos\bar{\alpha} + T_c \sin\alpha \tag{16}$$

Notice that for the case of no power ($C_T = T_c = 0$) then Eq. (16) reduces to

$$C_L = C_L^*(S_c/S) + (C_L^*)_{w-c}(1 - S_c/S)$$

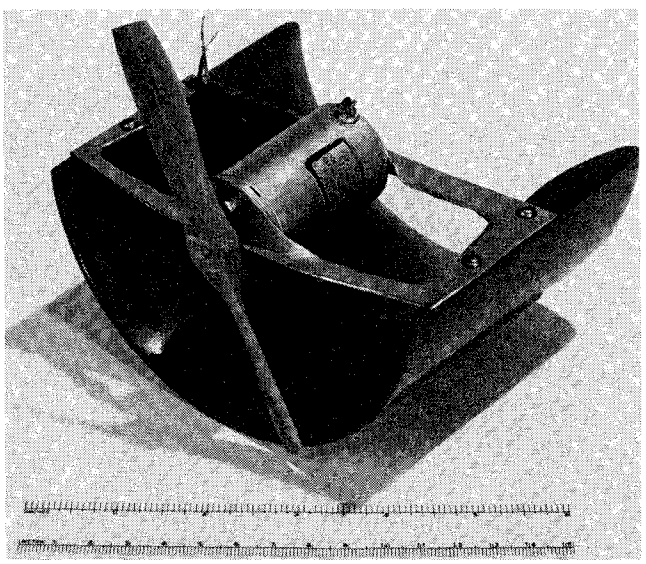

Fig. 6 Channel-wing wind-tunnel model.

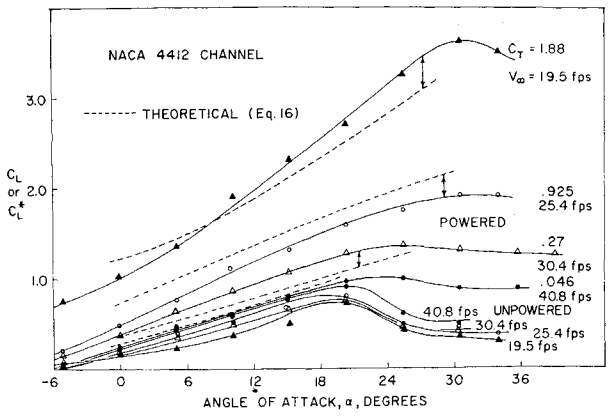

Fig. 7 Comparison between theory and small-scale wind-tunnel data.

Experimental Results

Figure 5 shows an application of the theory [Eq. (16)] to the full-scale wind-tunnel data of Ref. 1. The aircraft was a modified Piper Cub (empty weight = 900 lb) fitted with two Continental C-90 engines of approximately 90 hp each driving 6-ft-diam metal propellers mounted in two wing channels. For the wind-tunnel tests the two C-90 engines were replaced by two variable-speed electric motors. The data in Fig. 5 were obtained by operating the electric motors at 2450 rpm (170 hp total for both propellers). The static thrust at 2450 rpm was calculated to be 455 lb/propeller or 910 lb total. The projected area of channel wings S_c was 35 ft^2 and the total projected wing area S, (includes projected fuselage and channel wing area) was 59 ft^2.

All airfoil sections were NACA 4412. In the absence of data on the span-wise lift distribution, it was assumed that $C_L^* = (C_L^*)_{w-c}$ in Eq. (16). The data in Fig. 5 indicate that the theory correlates moderately well with the experimental data. Two of the reasons the theory underestimates the experimental data are 1) the experimental data includes the total lift of the horizontal tail plus the wing, while the theory includes only wing lift 2) the unpowered (C_L^*) lift distribution is not constant, as assumed by the theory in Fig. (5), hence the C_L^* for the channel areas is in all probability greater than the $(C_L^*)_{w-c}$ for the wing tips plus projected fuselage area.

It is interesting to note the lack of stall in the lift data in Fig. 5, even though the angles-of-attack ran up to 40°. The unpower lift data (C_L^*) of Ref. 1 had a constant slope of approximately 0.6 per degree up to $\alpha = 20°$, at which point the slope changed and C_L^* remained essentially constant at a value close to 1.3 up to the maximum angle of attack tested $\alpha = 35°$. The powered lift coefficients calculated by Eq. (16) in Fig. 5 were based on measured C_L^* values up to $\alpha = 20°$ and C_L^* values extrapolated from the unstalled lift curve slope for $\alpha > 20°$. This was done because it is apparent from the power-on lift tests that the channel did not stall, hence it would have been unrealistic to use stalled values of C_L^*.

A small wind-tunnel model of semicircular channel wing was constructed and tested in an AEROLAB Educational Wind Tunnel ($\frac{1}{2}$ hp). The channel wing model had an NACA 4412 section, a 5.5-in. chord and a 5.3-in. diam (see Fig. 6). Balsa was used as a construction material and was painted with filler and nitrate dope. The channel was turned on a lathe from a solid block and the resulting wing was cut in half. The engine used was a Globe Industries 27.5 VDC electric motor. A standard wood, 6-in.-diam, 5 pitch, top-flight model airplane propeller was cut down to 5.2-in. diam and press fitted on the motor shaft.

A comparison between power-on and power-off lift data is shown in Fig. 7. Again, a fair correlation is seen to exist be-

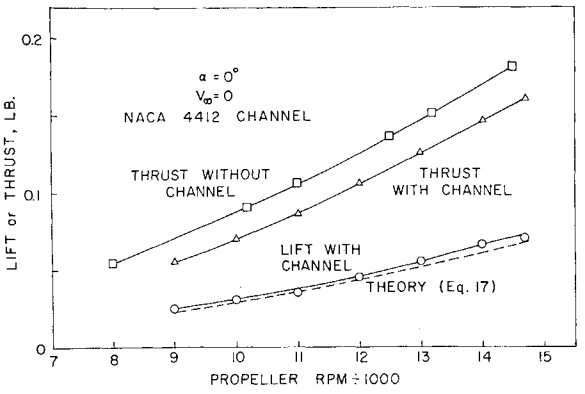

Fig. 8 Lift and thrust at zero forward speed.

tween the theory [Eq. (16)] and the test data. The maximum difference is about 12%. It is seen that adding power to the channel greatly increased the stalling angle of attack.

The unpowered lift coefficient data showed a strong Reynolds number (hence velocity) dependency. This was probably because of the fact that the Reynolds numbers were very low (i.e., $Re = 46{,}600$ at $V_\infty = 19.5$ fps).

Since it was not possible in these tests to isolate the thrust from the channel drag, the thrust coefficients used to calculate the theory curves [Eq. (16)] were based on measured thrust of the isolated propellers at the same rpm and tunnel speed. The extent of the error this introduces is not known, but it is probably less than 10%, if we can base our estimates on the thrust reductions because of the channel at zero tunnel speed. Figure 8 indicates that the propellers in the channels produced about 10% less thrust than the isolated propeller, at zero tunnel speed and $\alpha = 0°$.

The lift in the channel at zero forward speed can be determined from Eq. (15) to be

$$L_0 = (TS_c/4A)[(1 - \eta)C_L{}^* + \cos\bar{\alpha}] + nT\sin\alpha \quad (17)$$

The static lift data in Fig. 8 agrees very well with Eq. (17). A $C_L{}^*$ value of 0.1 was used for Eq. (17) in Fig. 8.

Accurate drag data were difficult to obtain in the small wind tunnel that was used. There was no readily available method for substracting out the interference drag and no method was available for measuring the true thrust of the propellers in the channels. Accordingly the drag data in Fig. 9 were obtained by substracting from the apparent drag reading the tare drag of the sting, and the measured thrust of the isolated propeller at the same rpm and tunnel speed. Figure 9 indicates that the apparent drag does increase with increasing thrust coefficient.

FAA-approved flight-test data[9] on the CCW-5 Custer channel wing airplane (Fig. 10) is plotted in Fig. 11. At the lowest speed flown, 42 mph, ($C_L = 4.9$) the airplane had not

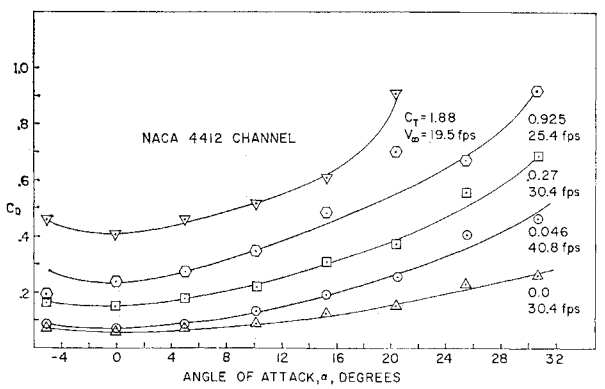

Fig. 9 Drag coefficient of small-scale wind-tunnel model.

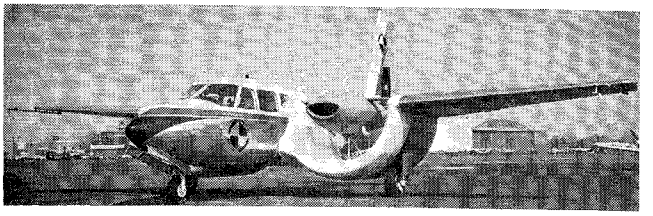

Fig. 10 Custer channel wing aircraft, CCW-5.

yet stalled. Theory [Eq. (16)] compares well with the data in Fig. 11 and predicts a $C_{L_{max.}} = 6.7(V_{stall} = 36\text{mph})$ at $\alpha = 40°$ and $C_T = 7.3$, assuming the necessary elevator power is available. Multiple-values of C_L can occur at fixed α, for multiple values of C_T.

Conclusions

From the wind-tunnel data, we conclude that the simple theory summarized by Eq. (16), can be used to make preliminary estimates of the lift developed by power-channel wings, with channel aspect ratios (diam/chord) in the neighbourhood of 1.0. Extremely large lift coefficients can be obtained with powered-channel wings.

Appendix: Evaluation of η

The pressure coefficient on the lower side of an airfoil can be expressed as[10]

$$C_{p_L} = 1 - [(u/V_\infty) - (\Delta u/V_\infty) - (C_l - C_{l_i})(\Delta u_a/V_\infty)]^2 \quad (A1)$$

Since the fraction of lift generated by the lower surface of the airfoil is given by

$$\eta = \cos\bar{\alpha}\int_0^1 C_{p_L}\,d(x/c)\Big/C_L{}^* \quad (A2)$$

then by substituting Eq. (A1) into Eq. (A2), η can be expressed as

$$\eta = \left(\frac{1}{C_L{}^*}\right)\cos\bar{\alpha}\int_0^1\left\{1 - \left[\frac{u}{V_\infty} - \frac{\Delta u}{V_\infty} - (C_l - C_{l_i})\frac{\Delta u_a}{V_\infty}\right]^2\right\}d(x/c) \quad (A3)$$

Values of u/V_∞, $\Delta u/V_\infty$, and $\Delta u_a/V_\infty$ represent the values of velocity on an airfoil because of the thickness, camber and

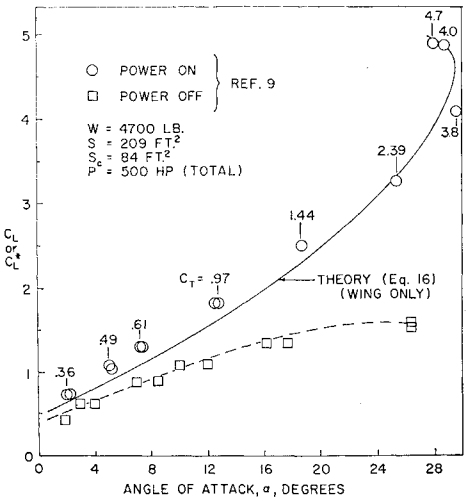

Fig. 11 Comparison between theory and flight-test data.

angle-of-attack, respectively and they can be obtained from tables in Ref. 10 for various NACA airfoils

References

[1] Pasamanick, J., "Langley Full-Scale-Tunnel Tests of The Custer Channel Wing Airplane," RM L53A09, April, 1953, NACA.

[2] Young, D. W., "Tests of Two Custer Channel Wings Having A Diameter of 37.2 Inches and Lengths of 43 and 17.5 Inches," AAF TR 5568, April 1947, AAF Air Material Command, Wright Field, Ohio.

[3] Young, D. W., "Custer U-Shaped Channel Wing," AAF Memorandum Rept. TSEAL-2-4568-3-2, July, 1945, AAF Air Technical Service Command, Engineering Div., Wright Field, Ohio.

[4] Young, D. W., "Test of $\frac{1}{3}$ Scale Powered Model of Custer Channel Shaped Wing-Five Foot Wind Tunnel Test No. 487," AAF TR 5142, Sept. 1944, AAF Material Center, Wright Field, Ohio.

[5] Crook, L. H., "Lift Forces On Custer Model Scoop With G-398 Airfoil Section," Aero. Rept. No. 571, Jan, 1944, L. H. Crook Aero. Lab., Catholic Univ., Washington, D. C.

[6] Crook, L. H., "Full Scale Static Lift Tests On Custer 72-inch Diameter Channel-Wing," Aero. Rept. 681, Dec. 1947, L. H. Crook Aero. Lab., Catholic Univ., Washington, D. C.

[7] Crook, L. H., "Full Scale Tests On CCW-2 Experimental Aircraft," Aero. Rept. 693, July 1951, L. H. Crook Aero. Lab., Catholic Univ., Washington, D. C.

[8] Dommasch, D. O., Sherby, S. S., and Connolly, T. F., *Airplane Aerodynamics*, 4th ed. Pitman, New York, 1967, p. 217.

[9] Robinson, A., "Flight Test And Theoretical Determination of Aerodynamic Coefficients of Custer Channel Wing Model CCW-5," June 1964, DES Rept. 507, De Vore Aviation Service, Roslyn Heights, N.Y.

[10] Abbott, I. A. and Von Doenhoff, A. E., *Theory of Wing Sections*, Dover, New York, 1958, pp. 77–78.

APRIL 1971 J. AIRCRAFT VOL. 8, NO. 4

Flight Path Optimization with Multiple Time Scales

HENRY J. KELLEY*
Analytical Mechanics Associates Inc., Jericho, N. Y.

The use of multiple time scales[1] in the optimization of aircraft flight paths is examined via asymptotic expansion in several parameters.[2,3] It turns out that, with more than two scales, the boundary layers develop their own boundary layers and the problem decouples into several problems of lower order, some furnishing performance indices for others. In the following example, optimal aircraft motion on three time scales is examined in cascaded boundary-layer approximation.

Introduction

THE idea of time-scale separation in vehicle dynamics is expounded in an excellent paper by Ashley[1] based upon asymptotic expansion techniques from fluid dynamics research, as reported in the references cited. The same intuitive insight regarding multiple time scales underlies the present treatment of optimal aircraft flight; however, the asymptotic methods of ordinary differential equations[2,3] are adopted. There appears to be a close conceptual kinship between the two bodies of literature but only limited cross-referencing. An earlier publication in the present vein has examined the aircraft "energy climb" and a related turning-flight approximation in terms of motion on two time scales[4]; another one has explored the adaptation of asymptotic expansion theory of ordinary differential equations to a simple variational two-point boundary-value problem.[5] The main point of the present paper is the decoupling of a high-order three-dimensional aircraft flight problem into several (specifically three) lower-order problems, with the possibility of further extension to rigid-body and control-motion problems which take place on additional, faster, time scales.

Asymptotic Expansion Formulation

The equations of motion for three-dimensional aircraft flight are

$$\epsilon_2\dot{h} = V\sin\gamma \tag{1}$$

$$\epsilon_2\dot{\gamma} = (g/V)[(L + \epsilon_2 T\sin\alpha)\cos\mu/(W_0 + \epsilon_2\Delta W) - \cos\gamma] \tag{2}$$

$$\epsilon_1\dot{E} = \{[(T - D)V + \epsilon_2 TV(\cos\alpha - 1)]/(W_0 + \epsilon_2\Delta W)\} \tag{3}$$

$$\epsilon_1\dot{\chi} = gL\sin\mu/V(W_0 + \epsilon_2\Delta W)\cos\gamma \tag{4}$$

$$\dot{x} = V\cos\gamma\sin\chi \tag{5}$$

$$\dot{y} = V\cos\gamma\cos\chi \tag{6}$$

$$\Delta\dot{W} = -Q(V,h) \tag{7}$$

These apply for full-throttle, zero side-force flight over a flat Earth. The right members incorporate, for $\epsilon_2 = 0$, the assumptions of constant weight and thrust directed along the path.[4] $E \equiv h + V^2/2g$ is specific energy, χ heading angle, γ path angle to horizontal, and μ bank angle. The symbol V for velocity should be regarded as merely convenient shorthand for $V \equiv [2g(E - h)]^{1/2}$.

An asymptotic expansion in the parameters ϵ_1 and ϵ_2, which fall in the ranges $0 \leq \epsilon_1 \leq 1$, $0 \leq \epsilon_2 \leq 1$, is contemplated. Following Tihonov,[2,3] it is supposed that the ratio $\epsilon_2/\epsilon_1 \to 0$ as $\epsilon_1 \to 0$. The parameters ϵ_1 and ϵ_2 are normalized analogues of the small parameters of fluid mechanics boundary-layer theory, e.g., in a flow problem ϵ might be defined as $\epsilon \equiv \nu/\bar{\nu}$, where ν is the viscosity and $\bar{\nu}$ its numerical value for a particular problem of interest. The hope of an expansion procedure is that the solutions sought for $\epsilon_i = 1$ differ little from those obtained for $\epsilon_i = 0$ except in short-time intervals of transition, "boundary layers" in an extended sense of the term.

The dependence of the *left* members of the system of state Eqs. (1–7) upon ϵ_1 and ϵ_2 is of primary importance in furnishing reductions in order. This order reduction with the vanishing ϵ_i is the defining feature of *singular perturbation problems.*

Received November 17, 1969; revision received August 17, 1970. Research performed under Contract NAS 12-656 with NASA Electronics Research Center, Cambridge, Mass.

* Vice President. Associate Fellow AIAA.